

Metabolomic profiling of human bladder tissue extracts

Krzysztof Ossoliński

John Paul II Hospital

Tomasz Ruman

Rzeszów University of Technology

Valérie Copié

Montana State University

Brian P. Tripet

Montana State University

Artur Kołodziej

Rzeszów University of Technology

Aneta Płaza-Altamer

Rzeszów University of Technology

Anna Ossolińska

John Paul II Hospital

Tadeusz Ossoliński

John Paul II Hospital

Anna Nieczaj

Rzeszów University of Technology

Joanna Nizioł (✉ jniziol@prz.edu.pl)


Rzeszów University of Technology

Research Article

Keywords: bladder cancer, biomarker, human tissue, metabolomics, NMR, laser mass spectrometry

Posted Date: May 30th, 2023

DOI: <https://doi.org/10.21203/rs.3.rs-2985696/v1>

License:  This work is licensed under a Creative Commons Attribution 4.0 International License. [Read Full License](#)

Additional Declarations: No competing interests reported.

Version of Record: A version of this preprint was published at Metabolomics on January 24th, 2024. See the published version at <https://doi.org/10.1007/s11306-023-02076-w>.

Abstract

Introduction

Bladder cancer is a common malignancy affecting the urinary tract and effective biomarkers and for which monitoring therapeutic interventions have yet to be identified.

Objectives

Major aim of this work was to perform metabolomic profiling of human bladder cancer and normal tissue and to evaluate cancer biomarkers

Methods

This study utilized nuclear magnetic resonance (NMR) and high-resolution nanoparticle-based laser desorption/ionization mass spectrometry (LDI-MS) methods to investigate polar metabolite profiles in tissue samples from 99 bladder cancer patients.

Results

Through NMR spectroscopy, six tissue metabolites were identified and quantified as potential indicators of bladder cancer, while LDI-MS allowed detection of 34 compounds which distinguished cancer tissue samples from normal tissue. Thirteen characteristic tissue metabolites were also found to differentiate bladder cancer tumor grades and thirteen metabolites were correlated with tumor stages. Receiver-Operating Characteristics analysis showed high predictive power for all three types of metabolomics data, with area under the curve (AUC) values greater than 0.853.

Conclusion

To date, this is the first study in which human normal tissues adjacent to cancerous tissues are analyzed. These findings suggest that the metabolite markers identified in this study may be useful for the detection and monitoring of bladder cancer stages and grades.

1. Introduction

Bladder cancer (BC), also known as urological or urinary bladder cancer, is the tenth most common and thirteenth most deadly cancer globally (sixth in men and seventeenth in women). According to the most recent GLOBOCAN data, BC accounts for approximately 3% of all cancer cases worldwide. Its prevalence is increasing, particularly in industrialized nations, with around 550,000 new cases diagnosed yearly (Sung et al. 2021). The incidence of bladder cancer rises with age, and the vast majority of cases (80%) occurs in those over 65. Moreover, males are four times more likely to be diagnosed with this disease than women. Environmental and occupational factors are responsible for most cases of bladder cancer, with the most significant risk being associated with tobacco smoke and being responsible for nearly 50% of bladder tumors; smokers are at a 2.5-fold higher risk than nonsmokers. Hereditary genetic predisposition causes 7% of cases of bladder cancer (Wong et al. 2018).

The bladder comprises urothelial cells, specialized transitional epithelial cells that collect urine, and smooth muscle that moves and excretes urine via the urethra to the outside. About 90% of BC arises from urothelial cells, mainly in the bladder, but in rare cases, also in the urinary tract (Saginala et al. 2020). This is due to their greater exposure to environmental, potentially mutagenic agents filtered into urine by the kidneys. These tumors have a relatively good prognosis (Mushtaq et al. 2019). The remaining 10% of BC are associated with a much worse prognosis and involve squamous cell carcinoma that affect smooth muscle cells. The World Health Organization classifies superficial bladder tumors as a heterogeneous category that includes urothelial papilloma (a benign lesion), papillary urothelial neoplasm of low malignant potential (PUNLMP), and low- and high-grade papillary malignancy. Around 75% of patients have non-muscle-invasive bladder cancer (NMIBC) with disease restricted to the mucosa (pTa, Tis) or lamina propria (pT1). The other 25% of newly diagnosed bladder tumors penetrate the muscularis propria bladder wall (pT2), called muscle-invasive bladder cancer (MIBC).

One of the first signs of urothelial malignancy is hematuria. It is often detected with a cystoscopy, telescopic endoscopy of the bladder, transabdominal ultrasonography, and/or computer tomography (CT) urography. Individuals with NMIBC are treated by transurethral resection of the bladder tumor (TURBT) and, for high-grade disease, with Bacillus Calmette-Guérin-based intravesical treatment (BCG, modified mycobacterium) (Sahu et al. 2017). While BCG helps delay or prevent the advancement of illness in a subset of individuals, a substantial number of patients ultimately acquire the invasive disease. Additionally, given the current global scarcity of BCG, this group needs alternate, sensitive therapy. Patients with muscle-invasive bladder cancer (MIBC) undergo radical cystectomy and bilateral, regional lymph node dissection, with or without preoperative chemotherapy or chemoradiation. The latest statistics from the American Cancer Society reveal in 2021 that the overall 5-year survival rate for bladder cancer in the United States is roughly 77%. Still, this figure varies significantly depending on the cancer stage at diagnosis (Siegel et al. 2022). If the cancer is localized and has not spread beyond the bladder, the 5-year survival rate is approximately 95%. On the other hand, if the bladder cancer has metastasized and spread to other parts of the body, the 5-year survival rate drops to about 5%. Early detection of cancer enables its resection and improved survival rates.

Despite significant efforts, no clinically viable biomarkers for early detection, diagnosis, or prognosis of BC are currently available. Analyzing the metabolic profiles of tissues and biofluids is a potential strategy for establishing robust small molecule indicators of BC, which would improve our ability to predict cancer progression and to evaluate the efficacy of cancer treatment.

Metabolomics is a modern and powerful technology, making it possible to detect compounds and determine previously unknown mechanisms related to disease progression (Zhang et al. 2020). By examining metabolites in biological samples such as urine (Jin et al. 2014), serum (Bansal et al. 2013), and tissue (Y. Cheng et al. 2015a), metabolomics tracks the metabolic response of living systems to disease or drug toxicity. The information obtained through metabolomic profiling studies on BC can potentially identify valuable biomarkers for diagnostic purposes and as indicators of cancer recurrence (Di Meo et al. 2022).

Over the last two decades, two analytical platforms have been used primarily for metabolomic analysis of diverse kidney cancer samples: mass spectrometry (MS) (Zeki et al. 2020) and nuclear magnetic resonance (NMR) (Emwas et al. 2019). To our knowledge, very few reports are available in the literature regarding human bladder tissue analysis. The first metabolomic profiling of bladder tissues was performed in 2011 by Putluri et

al. using LC-MS (Putluri et al. 2011). Analysis of 58 tissues revealed significantly changed levels of 35 mass spectral features within bladder tissues. Further research was carried out in 2013 by Tripathi et al. using the high-resolution magic angle spinning (MAS) NMR method. The findings revealed 22 distinct metabolites in different stages of BC. These results were cross-validated using targeted GC-MS analysis but did not include analysis of normal, unaffected tissues as controls (Tripathi et al. 2013). In a study published in 2017, Piyarathna et al. examined 165 tissues derived from the bladder, including 126 bladder cancer tissues and 39 benign or normal adjacent tissues. Based on UHPLC-HRMS analysis, they found 570 lipids associated with the survival and different clinical stages of BC (Piyarathna et al. 2018)

The present study employed two analytical platforms: NMR and LDI-MS, to investigate the metabolic changes in 198 human tissue samples of 99 BC cancer cases. This work aimed to characterize the most differentiating metabolites between cancer and normal tissues and also enabling the differentiation of cancer stages and grades. The discovery of significant metabolites provides clues at previously poorly understood or unknown metabolic changes that are associated with BC.

2. Materials and methods

2.1. Materials and equipment

All solvents were of 'LC-MS' grade and purchased from Sigma Aldrich (St. Louis, MO, USA). Deuterium oxide (D_2O) and DSS (4,4-dimethyl-4-silapentane-1-sulfonic acid) were purchased from Sigma Inc. (Boston, MA, USA).

2.2. Collection of human tissue samples

After comprehensive clinical questioning at John Paul II Hospital in Kolbuszowa, tissue samples were gathered from 99 patients with bladder cancer (20 females, 79 males, average age 72) receiving surgical therapy (Poland). The research was approved by the University of Rzeszow's local Bioethics Committee (Poland, permission number 2018/04/10) and followed all applicable rules and regulations. All the patients in this study were of the Caucasian race. Specimens and clinical data from patients involved in the study were collected with informed consent. All laboratory test results (complete blood count, bleeding profile, kidney function tests, CRP) were within normal ranges. Tissues for the metabolomic study were collected during a transurethral resection of a bladder tumor. For metabolomic study, we collected roughly cubic fragments of 2–4 mm size of the cancerous tumor and a fragment of normal bladder mucosa. Both of these fragments were cut in half, one part was taken for examination and the other was sent for histopathological examination to verify the diagnosis. Samples were immediately frozen and stored at $-60^{\circ}C$ until further use. The pathological and clinical characteristics of the patients are presented in the supplementary material table (Table S1).

2.3. Preparation of tissue metabolite extracts

As a result of the extraction of tissue samples, two fractions (phases) were obtained, the upper one containing medium-to-high polarity metabolites and the lower one containing low-polar metabolites. Detailed sample preparation protocols have been described in the Supplementary materials (Section S1) and our recent publication (Nizioł et al. 2021).

2.4. Analysis of tissue samples

Tissue extracts were analyzed using high-resolution ^1H NMR (upper phase) and silver-109 nanoparticle-based laser desorption/ionization mass spectrometry ($^{109}\text{AgNPs}$ -LDI-MS, upper and lower phase, analyzed separately). Silver-109 nanoparticles ($^{109}\text{AgNPs}$) were generated with pulsed fiber laser (PFL) 2D galvoscaner (2D GS) laser synthesis in solution/suspension (LASiS) as described in our previous publication (Płaza et al. 2021). Supplementary data detail the acquisition and processing of NMR and MS spectra (S2-S4).

2.5. Multivariate statistical analysis

MetaboAnalyst version 5.0 online software was used to analyze all metabolite datasets (Pang et al. 2021). The multivariate statistical analysis used here is similar to the one described in our recent publications (Nizioł et al. 2021, 2022; Ossoliński et al. 2022). Briefly, the metabolite data obtained from each analytical technique was log-transformed, auto-scaled, and normalized on the weight of the fresh tissue. The resulting metabolite profiles were then subjected to unsupervised Principal Component Analysis (PCA) and Orthogonal Partial Least Squares Discriminant Analysis (OPLS-DA). Metabolites which Variable Importance in Projection (VIP) values, associated with the OPLS-DA modeling, were greater than 1.0 were considered potentially significant discriminators of BC patients from normal controls (NCs). Permutation tests using 2000 steps were used to validate and assess the accuracy of the OPLS-DA models. Paired parametric t-test with Mann-Whitney and Bonferroni correction and fold change (FC) analysis were employed to evaluate the statistical significance of tissue metabolite level differences. Metabolites with P-values and false discovery rates (FDR) less than 0.05 and $\text{FC} > 2$ or < 0.5 were considered statistically significant (Benjamini et al. 2001). Furthermore, receiver operating characteristic curve (ROC) analyses were performed with random forest modeling to validate the OPLS-DA models and assess the metabolites' diagnostic value. Mass features identified by NMR and MS, respectively. Metabolite variables with an AUC (area under the curve) greater than 0.75 were deemed relevant to the discrimination of BC versus AN tissue metabolome. Training and validation metabolite datasets were subjected to independent multivariate statistical analyses. Compounds that separated tumors from control urine samples were chosen for external validation, which employed two independent datasets (here referred to as the training and validation datasets) to evaluate the performance of the OPLS-DA models (Ho et al. 2020). The established statistical criteria were applied to both training and validation datasets. A metabolic pathway impact analysis was performed using MetaboAnalyst 5.0 (Pang et al. 2021) and the Kyoto Encyclopedia of Genes and Genomes (Okuda et al. 2008) to identify metabolic pathways that are, in all likelihood, impacted by bladder cancer. To determine whether there were significant disparities in the average math test scores between different stages and grades of BC, we carried out a one-way analysis of variance (ANOVA) with Tukey's post-hoc testing.

3. Results

To uncover possible discriminant biomarkers of bladder cancer, 198 metabolite extracts from frozen bladder tissue samples (99 BC and 99 AN – 'adjacent normal') were examined using high-resolution 1D ^1H NMR and silver-109 nanoparticle-based laser desorption/ionization mass spectrometry ($^{109}\text{AgNPs}$ -LDI-MS).

3.1. Distinguishing between bladder cancer and normal tissues by ^1H NMR metabolomics

In total, 43 metabolites were identified and quantified in each tissue sample using ^1H NMR spectroscopy following published protocols (Nizioł et al. 2021). Figure 1 depicts an overlay of NMR spectra of cancer and normal tissue samples. Detailed spectra analysis revealed significant differences in metabolite levels between BC and AN tissues.

>>> Fig. 1 <<<

NMR datasets were randomly divided into two subsets: a training data set to train a model ($n = 69$ BC and $n = 69$ AN) and a validation data set to assess the validity and robustness of the learned model ($n = 30$ BC and $n = 30$ AN). Metabolite concentrations from both groups were statistically analyzed to assess whether differences in metabolite levels between cancer and normal tissue were significant. Findings from this analysis are reported in supplementary data Tables S2 and S3. Unsupervised score plots using PCA were generated for both subsets, revealing a poor distinction between BC and AN tissue. The most distinct separation between groups was identified using the first and second principal components, PC1 and PC2, which accounted for 48.8% and 10.0% of the variation in the training set, as shown in Fig. 2a. Similarly, in the validation set, a noticeable separation was observed between cancer and normal tissue samples along the first and second components, which accounted for 52.3% and 11.9%, respectively.

>>> Fig. 2 <<<

Subsequently, a supervised multivariate analysis was performed to investigate the metabolic distinctions between the BC and AN groups in both the training and validation sets, using OPLS-DA analysis. As depicted in Fig. 2b for the training set, and Fig. S1bin the supplementary data for the validation set, a distinct separation was observed between the two groups in the score plot. To confirm the reliability of the OPLS-DA model, two thousand permutation tests were conducted, and the statistical robustness of the model was verified, as shown in Table S4 in supplementary data. In the training set, there was good discrimination between the two groups ($Q^2 = 0.536$, $R^2Y = 0.682$, $P\text{-value} < 5E-04$ (0/2000)), revealing substantial differences in the metabolic profiles of BC vs AN tissues sample. The permutation test supported the group separations found with OPLS-DA in the validation set ($Q^2 = 0.287$, $R^2Y = 0.466$, $P\text{-value} < 5E-04$ (0/2000)).

To evaluate the diagnostic performance of the OPLS-DA models and to identify potential tissue polar metabolite biomarkers of bladder cancer, ROC analysis was conducted on both the training and validation datasets, along with the examination of VIP plots resulting from the OPLS-DA modeling. The paired parametric t-test with Mann-Whitney and Bonferroni correction was employed to investigate the statistical significance of metabolite level differences. A combined analysis of VIP scores (> 1.0), t-tests (FDR corrected $P\text{-values} < 0.05$), fold Change ($FC > 2.0$ or < 0.5), and AUC (> 0.75) of training and validation set metabolite data identified six tissue metabolites as significant discriminators of BC versus AN tissue, as presented in Table 1. These included lactate, glutamine, glutamate, hypoxanthine, serine, and threonine.

Table 1

Results of targeted quantitative study of potential BC biomarkers derived from ¹H NMR data of tissue samples (P-value 0.05; VIP > 1.0; FC > 2.0 or < 0.5)

Metabolite		VIP ^a	P-value ^b	FDR ^b	FC ^c	AUC	Spec. [%] ^d	Sens. [%] ^d
Lactate	Cancer	2.02	2.81E-10	1.21E-08	3.832	0.889	82	85
Glutamine	vs.	1.59	3.62E-08	2.59E-07	2.296	0.800	72	71
Glutamate	Normal	1.23	7.96E-08	4.28E-07	2.132	0.780	65	75
Hypoxanthine		1.39	7.87E-09	1.13E-07	2.109	0.754	65	78
Serine		1.31	1.30E-08	1.20E-07	2.625	0.753	59	84
Threonine		1.29	1.40E-08	1.20E-07	3.246	0.751	57	82
Lactate	HG BC vs. HG AN	2.45	5.16E-05	2.22E-03	3.780	0.864	88	77
Ethanolamine		1.54	3.64E-04	5.21E-03	2.285	0.714	69	73
Lactate	LG BC	1.75	6.34E-09	9.09E-08	4.341	0.922	88	91
Alanine	vs. LG AN	1.44	1.17E-06	6.28E-06	2.553	0.801	67	79
Choline		1.43	6.35E-05	1.37E-04	2.014	0.779	77	72
Glutamine		1.49	1.35E-07	8.29E-07	2.807	0.870	79	77
Hypoxanthine		1.31	4.94E-09	9.09E-08	2.309	0.816	74	77
Leucine		1.18	1.62E-06	7.75E-06	2.594	0.759	65	86
Methionine		1.42	2.26E-09	9.09E-08	4.348	0.812	72	84
Phenylalanine		1.22	2.30E-08	2.47E-07	3.647	0.764	63	79

^aVIP scores derived from OPLS-DA model; ^bP-value and FDR determined from Student's t-test, ^cfold change between cancer and control urine calculated from the concentration mean values for each group – cancer-to-normal ratio; ^dROC curve analysis for individual biomarkers. AN: adjacent normal; AUC: area under the curve; BC: bladder cancer; FC: fold change; FDR: false discovery rate; HG – high-grade; LG – low-grade; pT1 and pTa – high risk non-muscle invasive bladder cancer; pT2 – muscle invasive bladder cancer VIP: variable importance in projection scores.

Metabolite		VIP ^a	P-value ^b	FDR ^b	FC ^c	AUC	Spec. [%] ^d	Sens. [%] ^d
Serine		1.44	1.00E-07	7.95E-07	2.725	0.817	74	77
Threonine		1.40	1.11E-07	7.95E-07	2.888	0.789	60	91
Tyrosine		1.25	3.57E-06	1.53E-05	2.791	0.759	74	77
Lactate	pTa BC	1.84	2.57E-10	3.69E-09	4.560	0.928	88	86
Glutamine	vs. pTa AN	1.68	1.77E-09	1.52E-08	2.747	0.884	80	80
Serine		1.28	2.89E-09	2.07E-08	2.753	0.814	69	90
Hypoxanthine		1.32	1.43E-10	3.07E-09	2.334	0.809	65	88
Alanine		1.40	5.23E-08	2.81E-07	2.498	0.805	69	80
Methionine		1.35	8.76E-11	3.07E-09	4.140	0.804	71	86
Threonine		1.32	1.18E-09	1.27E-08	2.758	0.798	63	88
Choline		1.52	5.46E-06	1.24E-05	2.021	0.793	74	76
Aspartate		1.12	2.34E-06	6.69E-06	2.824	0.786	67	82
Ethanolamine		1.15	8.35E-07	2.76E-06	2.238	0.770	71	76
Phenylalanine		1.03	4.65E-09	2.86E-08	3.621	0.761	61	90
Tyrosine		1.13	7.30E-07	2.62E-06	2.599	0.755	71	82
Trimethylamine	pT1 BC vs. pT1 AN	2.09	9.65E-04	2.08E-02	0.429	0.832	84	58
Lactate		2.40	7.25E-05	3.12E-03	3.760	0.859	74	68

^aVIP scores derived from OPLS-DA model; ^bP-value and FDR determined from Student's t-test, ^cfold change between cancer and control urine calculated from the concentration mean values for each group – cancer-to-normal ratio; ^dROC curve analysis for individual biomarkers. AN: adjacent normal; AUC: area under the curve; BC: bladder cancer; FC: fold change; FDR: false discovery rate; HG – high-grade; LG – low-grade; pT1 and pTa – high risk non-muscle invasive bladder cancer; pT2 – muscle invasive bladder cancer VIP: variable importance in projection scores.

>>> Table 1 <<<

ROC studies and random forest modeling were performed to determine the diagnostic value of the six identified metabolites. The classification ROC model (as shown in Fig. 2c and Supplementary Fig. S1c) demonstrated that the combination of the differential levels of these six metabolites was a reliable discriminator in both data sets, with an AUC of over 0.853. The validity of the ROC model was confirmed by a permutation test with 1000 permutation steps resulting in a p-value below 0.001. The highest significance in the training set, with an AUC of over 0.80, was achieved for two metabolites: lactate (AUC = 0.889, specificity = 82%, and sensitivity = 85%), and glutamine (AUC = 0.800, specificity = 72%, and sensitivity = 71%). Box and whisker plots for selected metabolites are presented in Figs 2d-h. Table 1 summarizes the most important statistical parameters for these five metabolites identified by ^1H NMR as potential biomarkers of BC. These findings suggest that these six metabolites may have enhanced diagnostic potential and could be valuable indicators of malignant versus normal tissues of patients with bladder cancer when evaluated together.

3.2. Distinguishing between grades of bladder cancer and normal tissues based on ^1H NMR metabolite profiling analysis

To assess the potential of ^1H NMR metabolite profiles of tissue extracts to differentiate between different grades of BC and AN tissue, we performed PCA, OPLS-DA, and one-way ANOVA analysis on training and validation data sets. The analysis included 94 tissue samples from patients with high-grade (HG) and low-grade (LG) cancer, with three samples from a papillary urothelial neoplasm of low malignant potential (PUNLMP) patients excluded. The training data set ($n = 26$ HG BC and HG AN and $n = 43$ LG BC and AN) was used to train the PCA model. The validation data set ($n = 11$ HG BC and AN and $n = 15$ LG BC and AN) was used to verify the validity and robustness of the separate group clustering observed in the PCA model. In both the training and validation sets, PCA and OPLS-DA scores plots showed good separation between HG BC and HG AN tissue (Fig. 3a, b, S2 a, b in supplementary material).

>>> Fig. 3 <<<

In the HG BC vs. HG AN tissue OPLS-DA model, two metabolites, including lactate and ethanolamine, were considered significant (VIP > 1, P -value, FDR < 0.05, FC < 0.5 or > 2.0, AUC > 0.70) in both the training and validation sets (Table 1). The ROC model for classification (Fig. 3C) indicated that the collective concentrations of these two metabolites were a dependable differentiator with an AUC of 0.851. These compounds were found in significantly higher concentrations in the cancer tissue compared to the adjacent normal tissue. Analysis of LG BC vs. LG AN in the training and validation sets of the OPLS-DA model showed that eleven commonly identified compounds were important in separating the two groups (Table 1). PCA and OPLS-DA scores plots resulting from this analysis illustrate the extent of the separation of LG BC, from AN BC based on differential tissue metabolite profiles in the training and validation datasets (Fig. 3a-b and S3 a, b in supplementary data). Based on the results of univariate ROC curve analyses, we determined that these models have satisfactory diagnostic performance with AUC = 0.911 (Fig. 3c). Although PCA analysis was unable to separate the groups based on distinct tumor grades (data not shown), the cancer groups separated clearly from the AN group.

3.3. Distinguishing between stages of bladder cancer and normal tissues based on ^1H -NMR metabolite profiling

A ^1H NMR metabolomics study of tissue samples was also employed to evaluate whether unique metabolite patterns can help distinguish between stages of BC. We performed PCA, OPLS-DA, and non-parametric one-way ANOVA analyses on a total of 198 tissue extracts from 70 patients with pTa BC, 19 patients with pT1 BC, and 12 patients with pT2 BC. Due to insufficient patients with pT1 and pT2 malignancy, validation on a separate dataset was performed only for samples from patients with pTa BC. A training data set was created with $n = 49$ pTa BC and $n = 49$ AN tissue extracts. A validation data set with $n = 21$ pTa BC, and $n = 21$ AN tissue extracts.

The PCA and OPLS-DA score plots demonstrated a small but distinctive separation between normal and cancer tissue samples from patients with pTa stages of BC (Fig. 4a, b). The performance of this model was then evaluated using ROC analysis. The AUC value of 0.921 in the training set indicated very good classification and suggested that the model has a high probability of correctly classifying the samples with pTa BC and can be considered an effective classification tool. (Fig. 4c).

>>> Fig. 4 <<<

The score plots generated by PCA and OPLS-DA indicated a noticeable distinction between the cancerous and non-cancerous tissue samples obtained from patients diagnosed with pT1 stage BC (Fig. 4d, e). From the ROC plot (Fig. 4f), it can be seen that this model also provided a very high classification ability with an AUC value of 0.946). Based on the cut-off criteria ($FC > 2$ or < 0.5 , $VIP > 1$; $AUC > 0.75$, P -value and $FDR < 0.05$), finally, 12, and 2 metabolites appeared to be most relevant for sample distinction between pTa BC vs. AN, and pT1 BC vs. AN, respectively (Table 1). Unfortunately, in the case of tissue extracts from patients with stage pT2, obtaining a significant separation of cancer and regular groups was impossible. Also, comparing the three cancer stage groups (pT1 versus pTa versus pT2) revealed no statistically significant differences (data not shown).

3.4. Untargeted metabolic profiling of tissue using PFL-2D GS LASiS $^{109}\text{AgNPs}$ LDI-MS

Pulsed fiber laser ablation synthesis was employed to generate silver-109 nanoparticles in solution (PFL-2D GS LASiS $^{109}\text{AgNPs}$). These nanoparticles were then utilized for laser mass spectrometry-based profiling of BC and AN extracts. We analyzed the bladder tissue's polar and non-polar metabolite extracts separately and randomly divided the data into two subsets for statistical analysis. The training dataset included 69 bladder cancer (BC) and 69 normal (AN) tissue samples, while the validation dataset included 30 BC and 30 AN tissue samples. 355 and 299 common features were detected in the polar and non-polar extracts of tissue samples, respectively.

2D-PCA and OPLS-DA scores plots were generated from multivariate statistical analysis of the PFL-2D GS LASiS $^{109}\text{AgNPs}$ LDI-MS mass spectral features obtained from polar tissue extracts. These plots clearly distinguished the cancerous tissue from the normal tissue as a result of their distinct metabolite profiles, as shown in the Supplementary data. (Fig. S4). For the training dataset, the validation of the OPLS-DA model using 2000 permutations resulted in R^2Y and Q^2 values of 0.872 (P -value $< 5E04$) and 0.964 (P -value $< 5E04$) (Table S4, supplementary data), while R^2Y and Q^2 values of 0.807 (P -value $< 5E04$) and 0.983 (P -value $< 5E04$), respectively, were measured when analyzing the MS metabolomics data present in the validation dataset. This analysis was followed by univariate and multivariate ROC analysis for both training and validation datasets (Fig. S4, supplementary data). Supplementary data Fig. S4 provides a summary of all ROC curves generated from the analysis of the training and validation datasets, with a range of feature counts (i.e., 5, 10, 15, 25, 50

and 100), along with corresponding AUC values and confidence intervals. Notably, the 50-feature panel of model 5 in the training set and the 25-feature panel of model 4 in the validation set exhibited excellent discrimination power for BC diagnosis (AUC > 0.971), as illustrated in supplementary Fig. S4. Based on the cut-off criteria (FC > 2 or < 0.5, VIP > 1; AUC > 0.75, *P*-value and FDR < 0.05), finally, 97 *m/z* values appeared to be most relevant for sample distinction between cancer and normal tissue in both training and the validation datasets.

The mass spectral features obtained from non-polar tissue extracts generated from untargeted PFL-2D GS LASiS ¹⁰⁹AgNPs LDI-MS experiments were also analyzed using PCA and OPLS-DA to identify the mass spectral features that most differentiated control from normal tissue extracts from patients with BC, using both training and validation datasets (Fig. S5, supplementary data). The results of both PCA and OPLS-DA scores plots indicate a clear separation between cancer and normal groups in both the training and validation data subsets. This suggests that PFL-2D GS LASiS ¹⁰⁹AgNPs LDI-MS-based metabolite profiling of non-polar tissue extracts is an effective method for identifying characteristic metabolic differences that distinguish bladder cancer from control groups. The OPLS-DA model was validated using 2000 random permutation steps, which resulted in R²Y and Q² values of 0.773 (*P*-value < 5 E04) and 0.898 (*P*-value < 5E04), respectively, for the training dataset. Similarly, for the validation dataset, R²Y and Q² values of 0.730 (*P*-value < 5E04) and 0.971 (*P*-value < 5E04) were obtained (see Supplementary data, Table S4). Following the completion of the analysis, both univariate and multivariate ROC analyses were performed. Supplementary Fig. S5 summarizes all the ROC curves generated from the training and validation datasets, with a range of feature counts (i.e., five, ten, fifteen, twenty-five, fifty, and one hundred), along with corresponding AUC values and confidence intervals for each curve. The 15-feature panel of model 3 in the training dataset demonstrated the highest accuracy, while the 10-feature panel of model 2 in the validation dataset exhibited the highest accuracy. In both the training and validation sets, a total of 36 spectral features were identified in non-polar tissue extracts with VIP scores > 1.0, FDR-corrected *P*-value < 0.05, FC < 0.5 or > 2.0, and AUC > 0.75.

Subsequently, selected mass spectral features observed in the PFL-2D GS LASiS ¹⁰⁹AgNPs LDI-MS spectra of polar and non-polar tissue extracts were subjected to putative compound identification. This was accomplished by searching against various metabolite databases, including the Human Metabolome Database (HMDB) (Wishart et al. 2007), the MetaCyc Metabolic Pathway Database (Caspi et al. 2018) and the LIPID MAPS® Lipidomics Gateway (Sud et al. 2007). By comparing the spectral features observed in PFL-2D GS LASiS ¹⁰⁹AgNPs LDI-MS mass spectra with those of compounds present in the aforementioned databases, a total of 30 and 4 mass spectral features from polar and non-polar tissue extracts respectively were assigned putative metabolite IDs. Detailed information on these identified features is provided in Supplementary data Table S5.

Discussion

In this study, we performed targeted and untargeted metabolic profiling of tissues obtained from patients diagnosed with BC. Our objective was to generate distinctive metabolic signatures that could aid in early and accurate detection of BC using NMR and ¹⁰⁹AgNPs LDI-MS techniques. We performed targeted ¹H NMR analysis of normal and neoplastic tissues to identify a panel of 43 metabolites. Thirty-four of these compounds were present in higher concentrations and nine at lower concentrations in the cancer tissue compared to adjacent normal one (see Tables S2,3 in Supplementary data). The elevated levels of these 34 metabolites may indicate an increased synthesis of tumor-related metabolites that are secreted by cancer cells or changes in the

composition of non-cancerous tissues caused by tumor infiltration through the epithelial barrier. In addition, the presence of tumors may trigger inflammatory responses that contribute to the elevation of certain metabolites. The metabolomics data obtained through ^1H NMR analysis showed that six compounds exhibited higher concentrations in cancerous tissue than in normal tissue, and these compounds effectively differentiated between the two groups with significant discriminating power (Table 1). These included lactate, glutamine, glutamate, hypoxanthine, serine, and threonine.

Among the metabolites that effectively discriminated between cancerous and normal tissue samples, lactate emerged as a particularly significant biomolecule with a high VIP value. As the anion of a hydroxy carboxylic acid, lactate plays a key role in human metabolism and serves as a crucial energy reservoir (Rosenstein et al. 2018). By enabling the maintenance of ATP production and mitigating acidosis caused by ATP hydrolysis, lactate plays a vital function in cellular metabolism (Rosenstein et al. 2018). Furthermore, lactate has been identified as a significant contributor to acidosis in the tumor microenvironment (TME), which is associated with an acid-resistant phenotype that enables cancer cells to promote their own survival (Afonso et al. 2020). To sustain the uncontrolled growth and proliferation of cancer cells, including urothelial carcinoma cells, glycolysis is the primary source of energy. Consequently, a high glycolytic flux is dependent on the overexpression of genes related to glycolysis, which leads to the overproduction of pyruvate, alanine, and lactate (Massari et al. 2016). Research suggests that elevated lactate levels and acidification resulting from cancer cells and glycolytic metabolism can promote carcinogenesis by causing matrix degradation and cancer cell invasiveness (Gatenby et al. 2006). Furthermore, lactate has been implicated in metastasis and resistance to chemo-radiotherapy (Fischer et al. 2007). Due to its involvement in various metabolic pathways, lactate holds promise as a potential biomarker for cancer diagnosis and prognosis (Liu et al. 2016; Massari et al. 2016). Our study found that levels of lactate were significantly higher in cancer tissues compared to normal tissues in patients with BC. This aligns with previous findings from the analysis of urine and serum samples from BC patients using both NMR and LC-MS (Bansal et al. 2013; Wittmann et al. 2014). Additionally, Tripathi et al reported higher levels of lactate in tumor samples compared to benign disease in their studies of BC tissues also using NMR (Tripathi et al. 2013). These consistent results across different studies suggest that lactate could be a potential biomarker for BC diagnosis and monitoring.

The second most differentiating cancer group and the normal metabolite with the highest VIP value was glutamine. This compound is among the most abundant free amino acids in the body and plays a crucial role in the transport of nitrogen and maintaining acid-base balance (Hall et al. 1996). It is a primary energy source for rapidly dividing cells and is involved in excreting nitrogen compounds (Labow and Souba 2000). Furthermore, glutamine is metabolized to fuel the tricarboxylic acid (TCA) cycle, a vital process for obtaining energy (Deberardinis et al. 2007). Cancer cells heavily rely on glutamine as an energy substrate and use it to synthesize nucleotides and other amino acids (Wu et al. 2020). Studies on bladder cancer suggest that glutamine may promote tumor metabolism and increase the aggressiveness of cancer cells. However, the mechanisms and effects of glutamine metabolism in cancer are still being actively researched (Sun et al. 2019). More recently, further studies have provided knowledge of the potential use of glutamine as a biomarker for bladder cancer (Alba Loras et al. 2019a). Our findings, which demonstrate elevated levels of glutamine in tumor tissue, are in line with numerous prior studies that have revealed a significant increase in glutamine levels in serum and urine samples from bladder cancer patients in comparison to controls (Bansal et al. 2013; Wittmann et al. 2014). Furthermore, a previous NMR-based study of bladder cancer tissue also reported higher

glutamine levels in tumor tissue relative to benign disease (Tripathi et al. 2013). Furthermore, in time series metabolomics analyses of urine and serum samples obtained from bladder cancer patients pre- and post-resection, glutamine demonstrated significant potential in differentiating neoplastic samples from healthy ones (Gupta et al. 2020; Jacyna et al. 2022).

Another potentially important marker of BC is the glutamate, which is a fundamental metabolite in the human body derived from alpha-amino acid anions and is the conjugate base of glutamic acid. It contains anionic carboxyl groups and a cationic amino group and plays a crucial role in both normal and abnormal brain functioning, as well as in peripheral organs (Danbolt 2001). Cancer cells alter metabolic pathways, shifting glucose conversion towards pathways required for cell proliferation and leading to increased synthesis of proteins, including glutamine (Guin et al. 2014). This feature is consistent with the increased level of glutamate observed in the samples of diseased individuals, indicating that glutamate could be a useful biomarker for BC with high diagnostic value and the ability to report on disease recurrence (Y. Cheng et al. 2015b). This conclusion was also confirmed by our analysis, which found that the tissue level of glutamate is higher in cancer tissue than normal tissue. Similarly, Wittmann et al. found that urinary levels of glutamate were significantly elevated in patients with bladder cancer compared to healthy controls, indicating their potential as diagnostic biomarkers for the disease (Wittmann et al. 2014).

Hypoxanthine is a natural purine base that is produced during purine degradation and can be converted to xanthine and uric acid while generating reactive oxygen species through the action of the xanthine oxidase enzyme (Lawal and Adeloju 2012). Due to its diminutive and polar structure, hypoxanthine can easily accumulate in biological fluids and tissues, making it a potential indicator for medical diagnosis (Garg et al. 2022). Specifically, hypoxanthine is a significant product that is generated during the breakdown of nucleotides and can serve as a precursor of uric acid and is an intermediate in the breakdown of purines (Pasikanti et al. 2010). As such, its quantification is highly valuable for relevant clinical diagnoses (Dervisevic et al. 2016). Furthermore, increased levels of hypoxanthine are associated with decreased levels of uric acid, adenosine, and inosinic acid. In cancer cells, this pathway is often disrupted, leading to the accumulation of hypoxanthine. Therefore, the measurement of hypoxanthine levels can not only serve as a potential biomarker for medical diagnosis, but may also provide important information about the underlying metabolic changes in cancer cells (Rodrigues et al. 2016). In our studies, hypoxanthine levels were higher in cancer tissue compared to normal. This compound has also been previously detected in higher amounts in the urine and serum of BC patients and suggested to be a potential bladder cancer biomarker (Alberice et al. 2013; Gao et al. 2012; Hu et al. 2021; A. Loras et al. 2018; Tan et al. 2017; Wittmann et al. 2014).

Serine and threonine are amino acids that were also found to be in high concentrations in BC tissue compared to normal in our study. Serine is an endogenous amino acid that plays a significant role in various biosynthetic pathways in the human body, such as pyrimidine, purine, creatine, and porphyrin biosynthesis. Cancer cells utilize serine as the primary source of one-carbon units, which are necessary for the production of cellular components and proliferation (Newman and Maddocks 2017). Additionally, serine protease is involved in tumor invasion and metastasis in oncogenesis (Sanguedolce et al. 2015). On the other hand, threonine is an essential amino acid that is crucial for the formation of various building blocks of proteins, including tooth enamel, collagen, and elastin. It also plays an essential role in the nervous system and several metabolic pathways. Both serine and threonine are critical elements of a serine/threonine-protein kinase, which has been identified

as a potential biomarker for bladder cancer (Hentschel et al. 2021). The increased levels of both serine and threonine in our study were also observed by other researchers in blood serum (Amara et al. 2019; Vantaku et al. 2019) and also in urine (Kim et al. 2010).

Utilizing modified silver-109 targets in LDI-MS experiments enabled to measure the amount of polar and non-polar metabolites in tissue extracts. By employing this approach, analysis of tissue metabolites using MS allowed for the identification of 31 compounds that exhibited lower abundance in cancer tissue in comparison to normal while one compound was found to be present in higher concentrations. Most of these compounds were putatively identified as peptides and lipids. Among the lipids found to be elevated in the normal tissue of BC patients, five belonged to the fatty acyl class, while the remaining three were classified as diradylglycerols, and one as a glycerophosphocholine.

The level of lipids in cancerous tissues can be influenced by various factors, including altered metabolism, changes in lipid transport and uptake, and increased utilization of lipids for energy production (C. Cheng et al. 2018). Cancer cells tend to exhibit increased aerobic glycolysis, also known as the Warburg effect, which can result in a reduction of lipid biosynthesis and accumulation in the cells (Broadfield et al. 2021). Additionally, cancer cells may rely on increased uptake of lipids from the extracellular environment to support their growth and proliferation. Moreover, cancer cells can utilize lipids as an energy source, which may contribute to a decrease in lipid levels in the tissue (Menendez and Lupu 2007).

In an effort to identify cellular markers that could distinguish between the various grades and stages of BC, several metabolomics studies of urine and blood of BC patients have been reported (Di Meo et al. 2022; Petrella et al. 2021). To our knowledge, however, only three studies have investigated the connections between changes in metabolite levels in tissues from BC patients and the distinct grades and/or stages of tumor development (Piyarathna et al. 2018; Sahu et al. 2017; Tripathi et al. 2013).

In our study, significantly higher concentrations of lactate and ethanolamine were measured in the HG cancer tissue of BC patients compared to the levels found in the normal tissue group (Fig. 3, Table 1). We found that lactate is one of the most differentiating metabolites between normal and neoplastic tissue, regardless of the stage of cancer. Ethanolamine is a component of certain phospholipids that make up the structure of cell membranes and plays an important role in the structure and function of cell membranes. These lipids are also involved in cell signaling and other cellular processes (Vance and Tasseva 2013). In some types of cancer, there is evidence that the levels of ethanolamine differ significantly between samples collected from cancer patients compared to controls (Swanson et al. 2008). The higher level of ethanolamine may be related to the increased cell proliferation and growth that is characteristic of cancer. Cancer cells may require more ethanolamine to support the synthesis of new cell membranes and other cellular structures as they divide and multiply (M. Cheng et al. 2016).

Our research has identified a panel of 11 metabolites that, when considered together, may be good discriminators of low-grade cancer tissue versus adjacent normal tissue in bladder cancer patients. These metabolites include lactate, alanine, choline, glutamine, hypoxanthine, leucine, methionine, phenylalanine, serine, threonine, and tyrosine, eight of which are alpha-amino acids.

One of the most differentiating compounds between LG cancer and normal tissue from BC patients is choline. It is a crucial water-soluble quaternary amine that is often classified as a B vitamin due to its similar chemical structure. Choline has several important functions within the human body, particularly in neurochemical processes (Tayebati et al. 2017). Choline plays a critical role in the production of phospholipids and the metabolism of triglycerides, making it essential for the proper structure and function of cell membranes. Our study found that cancer tissue from patients with bladder cancer had higher levels of choline compared to normal tissue, which could be due to increased absorption of choline by cancer cells. Our findings are consistent with previous research demonstrating that cancer cells tend to increase fatty acid synthesis, which can then act as a substrate for phosphatidylcholine synthesis, leading to its elevation in tumor cells (Koundouros and Pouligiannis 2019; Saito et al. 2022). Interestingly, we observed the same trend in urine samples, with increased levels of choline observed in patients with BC (Li et al. 2021; Alba Loras et al. 2019b). Moreover, one of our previous studies revealed that the increase in tissue choline levels among cancer patients is consistent with the decrease in choline levels found in the serum of patients with BC compared to control individuals (Ossoliński et al. 2022).

Our current study has indicated that tissue-based metabolite profiling can accurately discriminate different stages of cancer tissue (pTa and pT1) from normal tissue from BC patients (Table 1, Fig. 4). In the tissue extracts of patients with pTa and pT1 stages of BC, we identified 13 significant metabolites that were good discriminators of the different cancer stage groups compared to the normal tissue group, most of which are alpha-amino acids and have also been reported in the literature, as described above, in relation to the occurrence of cancer.

Conclusion

Our study has demonstrated that the combination of multivariate statistics, high-resolution NMR, and silver-109-based high-resolution LDI-MS metabolomics can effectively identify changes in tissue metabolome of patients with bladder cancer (BC). Using ^1H NMR metabolomics, we identified six potentially robust metabolic indicators of BC, including lactate, glutamine, glutamate, hypoxanthine, serine, and threonine, which predicted BC with very good predictive power (AUC values > 0.853). Furthermore, using silver-109 nanoparticle-based LDI-MS, we identified 34 additional compounds, mostly lipids, that helped differentiate between cancer and normal tissues. Additionally, we found thirteen metabolites that could potentially discriminate between low-grade and high-grade bladder cancer and thirteen metabolites that could serve as potential reporters of different grades of BC. Overall, our findings suggest that a combination of tissue metabolites has better predictive potential for diagnosing BC and evaluating disease severity and progression than using individual metabolites alone.

Declarations

Author contributions

Investigation: KO, TR, AP, AK, JN; Methodology: KO, TR, JN; Resources: KO, TR, VC, BPT, AO, TO, JN; Data Curation: TR, VC, BPT, JN, AK, AP; Formal analysis: JN; Visualization: JN, BPT; Writing - Original Draft: KO, AN, JN; Writing - Review & Editing: VC, TR, BPT, JN; Supervision: JN, TR; Funding acquisition: JN, BPT, VC; Project administration: JN

Consent to participate

The patients provided written consent for participate in research.

Consent for publication

The patients provided written informed consent for the publication of any associated data.

Ethical approval

The study protocol was approved by local Bioethics Committee at the University of Rzeszow (Poland) (permission no. 2018/04/10).

Research involving human and/or animal participants

This article does not contain any studies with human and/or animal participants performed by either of the authors.

Conflict of interest

The authors declare no competing financial and/or non-financial interests.

Data Availability

The data that support the findings of this study are available from the corresponding author upon reasonable request.

Acknowledgments

Research was supported mainly by National Science Centre (Poland), research project SONATA Number UMO-2018/31/D/ST4/00109. ¹H NMR spectra were recorded at Montana State University-Bozeman on a cryoprobe-equipped 600 MHz (14 Tesla) AVANCE III solution NMR spectrometer housed in MSU's NMR Center. Funding for MSU NMR Center's NMR instruments has been provided in part by the NIH SIG program (1S10RR13878 and 1S10RR026659), the National Science Foundation (NSF-MRI:DBI-1532078, NSF-MRI CHE: 2018388), the Murdock Charitable Trust Foundation (2015066:MNL), and support from the office of the Vice President for Research, Economic Development, and Graduate Education at MSU.

References

1. Afonso, J., Santos, L. L., Longatto-Filho, A., & Baltazar, F. (2020). Competitive glucose metabolism as a target to boost bladder cancer immunotherapy. *Nature Reviews Urology* 2020 17:2, 17(2), 77–106. <https://doi.org/10.1038/s41585-019-0263-6>
2. Alberice, J. V., Amaral, A. F. S., Armitage, E. G., Lorente, J. A., Algaba, F., Carrilho, E., et al. (2013). Searching for urine biomarkers of bladder cancer recurrence using a liquid chromatography–mass spectrometry and capillary electrophoresis–mass spectrometry metabolomics approach. *Journal of Chromatography A*, 1318, 163–170. <https://doi.org/10.1016/J.CHROMA.2013.10.002>

3. Amara, C. S., Ambati, C. R., Vantaku, V., Piyarathna, D. W. B., Donepudi, S. R., Ravi, S. S., et al. (2019). Serum metabolic profiling identified a distinct metabolic signature in bladder cancer smokers: A key metabolic enzyme associated with patient survival. *Cancer Epidemiology Biomarkers and Prevention*, *28*(4), 770–781. <https://doi.org/10.1158/1055-9965.EPI-18-0936/70061/AM/SERUM-METABOLIC-PROFILING-IDENTIFIED-A-DISTINCT>
4. Bansal, N., Gupta, A., Mitash, N., Shakya, P. S., Mandhani, A., Mahdi, A. A., et al. (2013). Low- and high-grade bladder cancer determination via human serum-based metabolomics approach. *Journal of Proteome Research*, *12*(12), 5839–5850. https://doi.org/10.1021/PR400859W/SUPPL_FILE/PR400859W_SI_001.PDF
5. Benjamini, Y., Drai, D., Elmer, G., Kafkafi, N., & Golani, I. (2001). Controlling the false discovery rate in behavior genetics research. *Behavioural Brain Research*, *125*(1–2), 279–284. [https://doi.org/10.1016/S0166-4328\(01\)00297-2](https://doi.org/10.1016/S0166-4328(01)00297-2)
6. Broadfield, L. A., Pane, A. A., Talebi, A., Swinnen, J. V., & Fendt, S. M. (2021). Lipid metabolism in cancer: New perspectives and emerging mechanisms. *Developmental Cell*, *56*(10), 1363–1393. <https://doi.org/10.1016/J.DEVCEL.2021.04.013>
7. Caspi, R., Billington, R., Fulcher, C. A., Keseler, I. M., Kothari, A., Krummenacker, M., et al. (2018). The MetaCyc database of metabolic pathways and enzymes. *Nucleic Acids Research*, *46*(D1), D633–D639. <https://doi.org/10.1093/nar/gkx935>
8. Cheng, C., Geng, F., Cheng, X., & Guo, D. (2018). Lipid metabolism reprogramming and its potential targets in cancer. *Cancer Communications 2018 38:1*, *38*(1), 1–14. <https://doi.org/10.1186/S40880-018-0301-4>
9. Cheng, M., Bhujwalla, Z. M., & Glunde, K. (2016). Targeting phospholipid metabolism in cancer. *Frontiers in Oncology*, *6*(DEC), 266. <https://doi.org/10.3389/FONC.2016.00266/BIBTEX>
10. Cheng, Y., Yang, X., Deng, X., Zhang, X., Li, P., Tao, J., et al. (2015a). Metabolomics in bladder cancer: a systematic review. *International journal of clinical and experimental medicine*, *8*(7), 11052–63. <http://www.ncbi.nlm.nih.gov/pubmed/26379905> <http://www.pubmedcentral.nih.gov/articlerender.fcgi?artid=PMC4565288>
11. Cheng, Y., Yang, X., Deng, X., Zhang, X., Li, P., Tao, J., et al. (2015b). Metabolomics in bladder cancer: a systematic review. *International Journal of Clinical and Experimental Medicine*, *8*(7), 11052. </pmc/articles/PMC4565288/>. Accessed 18 April 2023
12. Danbolt, N. C. (2001). Glutamate uptake. *Progress in Neurobiology*, *65*(1), 1–105. [https://doi.org/10.1016/S0301-0082\(00\)00067-8](https://doi.org/10.1016/S0301-0082(00)00067-8)
13. Deberardinis, R. J., Mancuso, A., Daikhin, E., Nissim, I., Yudkoff, M., Wehrli, S., & Thompson, C. B. (2007). Beyond aerobic glycolysis: Transformed cells can engage in glutamine metabolism that exceeds the requirement for protein and nucleotide synthesis. www.pnas.org/cgi/content/full/. Accessed 18 April 2023
14. Dervisevic, M., Dervisevic, E., Azak, H., Çevik, E., Şenel, M., & Yildiz, H. B. (2016). Novel amperometric xanthine biosensor based on xanthine oxidase immobilized on electrochemically polymerized 10-[4H-dithieno(3,2-b:2',3'-d)pyrrole-4-yl]decane-1-amine film. *Sensors and Actuators B: Chemical*, *225*, 181–187. <https://doi.org/10.1016/J.SNB.2015.11.043>
15. Di Meo, N. A., Loizzo, D., Pandolfo, S. D., Autorino, R., Ferro, M., Porta, C., et al. (2022). Metabolomic Approaches for Detection and Identification of Biomarkers and Altered Pathways in Bladder Cancer.

- International Journal of Molecular Sciences*, 23(8), 4173. <https://doi.org/10.3390/IJMS23084173/S1>
16. Emwas, A. H., Roy, R., McKay, R. T., Tenori, L., Saccenti, E., Nagana Gowda, G. A., et al. (2019). NMR Spectroscopy for Metabolomics Research. *Metabolites* 2019, Vol. 9, Page 123, 9(7), 123. <https://doi.org/10.3390/METABO9070123>
 17. Fischer, K., Hoffmann, P., Voelkl, S., Meidenbauer, N., Ammer, J., Edinger, M., et al. (2007). Inhibitory effect of tumor cell-derived lactic acid on human T cells. *Blood*, 109(9), 3812–3819. <https://doi.org/10.1182/BLOOD-2006-07-035972>
 18. Gao, H., Dong, B., Jia, J., Zhu, H., Diao, C., Yan, Z., et al. (2012). Application of ex vivo ¹H NMR metabonomics to the characterization and possible detection of renal cell carcinoma metastases. *Journal of Cancer Research and Clinical Oncology*, 138(5), 753–761. <https://doi.org/10.1007/s00432-011-1134-6>
 19. Garg, D., Singh, M., Verma, N., & Monika. (2022). Review on recent advances in fabrication of enzymatic and chemical sensors for hypoxanthine. *Food Chemistry*, 375, 131839. <https://doi.org/10.1016/J.FOODCHEM.2021.131839>
 20. Gatenby, R. A., Gawlinski, E. T., Gmitro, A. F., Kaylor, B., & Gillies, R. J. (2006). Acid-mediated tumor invasion: a multidisciplinary study. *Cancer research*, 66(10), 5216–5223. <https://doi.org/10.1158/0008-5472.CAN-05-4193>
 21. Guin, S., Pollard, C., Ru, Y., Lew, C. R., Duex, J. E., Dancik, G., et al. (2014). Role in Tumor Growth of a Glycogen Debranching Enzyme Lost in Glycogen Storage Disease. *JNCI: Journal of the National Cancer Institute*, 106(5). <https://doi.org/10.1093/JNCI/DJU062>
 22. Gupta, A., Bansal, N., Mitash, N., Kumar, D., Kumar, M., Sankhwar, S. N., et al. (2020). NMR-derived targeted serum metabolic biomarkers appraisal of bladder cancer: A pre- and post-operative evaluation. *Journal of Pharmaceutical and Biomedical Analysis*, 183, 113134. <https://doi.org/10.1016/J.JPBA.2020.113134>
 23. Hall, J. C., Heel, K., & McCauley, R. (1996). Glutamine. *The British journal of surgery*, 83(3), 305–312. <https://doi.org/10.1002/BJS.1800830306>
 24. Hentschel, A. E., van der Toom, E. E., Vis, A. N., Ket, J. C. F., Bosschieter, J., Heymans, M. W., et al. (2021). A systematic review on mutation markers for bladder cancer diagnosis in urine. *BJU International*, 127(1), 12–27. <https://doi.org/10.1111/BJU.15137>
 25. Ho, S. Y., Phua, K., Wong, L., & Bin Goh, W. W. (2020). Extensions of the External Validation for Checking Learned Model Interpretability and Generalizability. *Patterns*, 1(8), 100129. <https://doi.org/10.1016/J.PATTER.2020.100129>
 26. Hu, D., Xu, X., Zhao, Z., Li, C., Tian, Y., Liu, Q., et al. (2021). Detecting urine metabolites of bladder cancer by surface-enhanced Raman spectroscopy. *Spectrochimica Acta - Part A: Molecular and Biomolecular Spectroscopy*, 247, 119108. <https://doi.org/10.1016/j.saa.2020.119108>
 27. Jacyna, J., Kordalewska, M., Artymowicz, M., Markuszewski, M., Matuszewski, M., & Markuszewski, M. J. (2022). Pre- and Post-Resection Urine Metabolic Profiles of Bladder Cancer Patients: Results of Preliminary Studies on Time Series Metabolomics Analysis. *Cancers* 2022, Vol. 14, Page 1210, 14(5), 1210. <https://doi.org/10.3390/CANCERS14051210>
 28. Jin, X., Yun, S. J., Jeong, P., Kim, I. Y., Kim, W. J., & Park, S. (2014). Diagnosis of bladder cancer and prediction of survival by urinary metabolomics. *Oncotarget*, 5(6), 1635. <https://doi.org/10.18632/ONCOTARGET.1744>

29. Kim, J. W., Lee, G., Moon, S. M., Park, M. J., Hong, S. K., Ahn, Y. H., et al. (2010). Metabolomic screening and star pattern recognition by urinary amino acid profile analysis from bladder cancer patients. *Metabolomics*, *6*(2), 202–206. <https://doi.org/10.1007/s11306-010-0199-6>
30. Koundouros, N., & Poulogiannis, G. (2019). Reprogramming of fatty acid metabolism in cancer. *British Journal of Cancer* *2019 122:1*, *122*(1), 4–22. <https://doi.org/10.1038/s41416-019-0650-z>
31. Labow, B. I., & Souba, W. W. (2000). Glutamine. *World Journal of Surgery*, *24*(12), 1503–1513. <https://doi.org/10.1007/S002680010269/METRICS>
32. Lawal, A. T., & Adeloju, S. B. (2012). Progress and recent advances in fabrication and utilization of hypoxanthine biosensors for meat and fish quality assessment: A review. *Talanta*, *100*, 217–228. <https://doi.org/10.1016/J.TALANTA.2012.07.085>
33. Li, J., Cheng, B., Xie, H., Zhan, C., Li, S., & Bai, P. (2021). Bladder cancer biomarker screening based on non-targeted urine metabolomics. *International Urology and Nephrology* *2021 54:1*, *54*(1), 23–29. <https://doi.org/10.1007/S11255-021-03080-6>
34. Liu, X., Yao, D., Liu, C., Cao, Y., Yang, Q., Sun, Z., & Liu, D. (2016). Overexpression of ABCC3 promotes cell proliferation, drug resistance, and aerobic glycolysis and is associated with poor prognosis in urinary bladder cancer patients. *Tumor Biology*, *37*(6), 8367–8374. <https://doi.org/10.1007/S13277-015-4703-5/FIGURES/4>
35. Loras, A., Trassierra, M., Sanjuan-Herráez, D., Martínez-Bisbal, M. C., Castell, J. V., Quintás, G., & Ruiz-Cerdá, J. L. (2018). Bladder cancer recurrence surveillance by urine metabolomics analysis. *Scientific Reports*, *8*(1), 1–10. <https://doi.org/10.1038/s41598-018-27538-3>
36. Loras, Alba, Suárez-Cabrera, C., Martínez-Bisbal, M. C., Quintás, G., Paramio, J. M., Martínez-Máñez, R., et al. (2019a). Integrative metabolomic and transcriptomic analysis for the study of bladder cancer. *Cancers*, *11*(5). <https://doi.org/10.3390/cancers11050686>
37. Loras, Alba, Suárez-Cabrera, C., Martínez-Bisbal, M. C., Quintás, G., Paramio, J. M., Martínez-Máñez, R., et al. (2019b). Integrative Metabolomic and Transcriptomic Analysis for the Study of Bladder Cancer. *Cancers* *2019, Vol. 11, Page 686*, *11*(5), 686. <https://doi.org/10.3390/CANCERS11050686>
38. Massari, F., Ciccarese, C., Santoni, M., Iacovelli, R., Mazzucchelli, R., Piva, F., et al. (2016). Metabolic phenotype of bladder cancer. *Cancer Treatment Reviews*, *45*, 46–57. <https://doi.org/10.1016/J.CTRV.2016.03.005>
39. Menendez, J. A., & Lupu, R. (2007). Fatty acid synthase and the lipogenic phenotype in cancer pathogenesis. *Nature Reviews Cancer* *2007 7:10*, *7*(10), 763–777. <https://doi.org/10.1038/nrc2222>
40. Mushtaq, J., Thurairaja, R., & Nair, R. (2019). Bladder cancer. *Surgery (Oxford)*, *37*(9), 529–537. <https://doi.org/10.1016/J.MPSUR.2019.07.003>
41. Newman, A. C., & Maddocks, O. D. K. (2017). Serine and Functional Metabolites in Cancer. *Trends in Cell Biology*, *27*(9), 645–657. <https://doi.org/10.1016/J.TCB.2017.05.001>
42. Nizioł, J., Copié, V., Tripet, B. P., Nogueira, L. B., Nogueira, K. O. P. C., Ossoliński, K., et al. (2021). Metabolomic and elemental profiling of human tissue in kidney cancer. *Metabolomics*, *17*(3), 30. <https://doi.org/10.1007/S11306-021-01779-2>
43. Nizioł, J., Ossoliński, K., Płaza-Altamer, A., Kołodziej, A., Ossolińska, A., Ossoliński, T., & Ruman, T. (2022). Untargeted ultra-high-resolution mass spectrometry metabolomic profiling of blood serum in bladder

- cancer. *Scientific Reports* 2022 12:1, 12(1), 1–13. <https://doi.org/10.1038/s41598-022-19576-9>
44. Okuda, S., Yamada, T., Hamajima, M., Itoh, M., Katayama, T., Bork, P., et al. (2008). KEGG Atlas mapping for global analysis of metabolic pathways. *Nucleic Acids Research*, 36(suppl_2), W423–W426. <https://doi.org/10.1093/NAR/GKN282>
45. Ossoliński, K., Ruman, T., Copié, V., Tripet, B. P., Nogueira, L. B., Nogueira, K. O. P. C., et al. (2022). Metabolomic and elemental profiling of blood serum in bladder cancer. *Journal of Pharmaceutical Analysis*, 12(6), 889–900. <https://doi.org/10.1016/J.JPHA.2022.08.004>
46. Pang, Z., Chong, J., Zhou, G., De Lima Morais, D. A., Chang, L., Barrette, M., et al. (2021). MetaboAnalyst 5.0: narrowing the gap between raw spectra and functional insights. *Nucleic Acids Research*, 49(W1), W388–W396. <https://doi.org/10.1093/NAR/GKAB382>
47. Pasikanti, K. K., Esuvaranathan, K., Ho, P. C., Mahendran, R., Kamaraj, R., Wu, Q. H., et al. (2010). Noninvasive urinary metabolomic diagnosis of human bladder cancer. *Journal of Proteome Research*, 9(6), 2988–2995. <https://doi.org/10.1021/PR901173V>
48. Petrella, G., Ciufolini, G., Vago, R., & Cicero, D. O. (2021). Urinary Metabolic Markers of Bladder Cancer: A Reflection of the Tumor or the Response of the Body? *Metabolites* 2021, Vol. 11, Page 756, 11(11), 756. <https://doi.org/10.3390/METABO11110756>
49. Piyaathna, D. W. B., Rajendiran, T. M., Putluri, V., Vantaku, V., Soni, T., von Rundstedt, F. C., et al. (2018). Distinct Lipidomic Landscapes Associated with Clinical Stages of Urothelial Cancer of the Bladder. *European Urology Focus*, 4(6), 907–915. <https://doi.org/10.1016/J.EUF.2017.04.005>
50. Płaza, A., Kołodziej, A., Nizioł, J., & Ruman, T. (2021). Laser Ablation Synthesis in Solution and Nebulization of Silver-109 Nanoparticles for Mass Spectrometry and Mass Spectrometry Imaging. *ACS Measurement Science Au*, 2(1), 14–22. <https://doi.org/10.1021/ACSMEASURESCIAU.1C00020>
51. Putluri, N., Shojaie, A., Vasu, V. T., Vareed, S. K., Nalluri, S., Putluri, V., et al. (2011). Metabolomic Profiling Reveals Potential Markers and Bioprocesses Altered in Bladder Cancer Progression. *Cancer Research*, 71(24), 7376–7386. <https://doi.org/10.1158/0008-5472.CAN-11-1154>
52. Rodrigues, D., Jerónimo, C., Henrique, R., Belo, L., De Lourdes Bastos, M., De Pinho, P. G., & Carvalho, M. (2016). Biomarkers in bladder cancer: A metabolomic approach using in vitro and ex vivo model systems. *International Journal of Cancer*, 139(2), 256–268. <https://doi.org/10.1002/IJC.30016>
53. Rosenstein, P. G., Tennent-Brown, B. S., & Hughes, D. (2018). Clinical use of plasma lactate concentration. Part 1: Physiology, pathophysiology, and measurement. *Journal of Veterinary Emergency and Critical Care*, 28(2), 85–105. <https://doi.org/10.1111/VEC.12708>
54. Saginala, K., Barsouk, A., Aluru, J. S., Rawla, P., Padala, S. A., & Barsouk, A. (2020). Epidemiology of Bladder Cancer. *Medical Sciences*, 8(1). <https://doi.org/10.3390/MEDSCI8010015>
55. Sahu, D., Lotan, Y., Wittmann, B., Neri, B., & Hansel, D. E. (2017). Metabolomics analysis reveals distinct profiles of nonmuscle-invasive and muscle-invasive bladder cancer. *Cancer Medicine*, 6(9), 2106–2120. <https://doi.org/10.1002/CAM4.1109>
56. Saito, R. de F., Andrade, L. N. de S., Bustos, S. O., & Chammas, R. (2022). Phosphatidylcholine-Derived Lipid Mediators: The Crosstalk Between Cancer Cells and Immune Cells. *Frontiers in Immunology*, 0, 215. <https://doi.org/10.3389/FIMMU.2022.768606>

57. Sanguedolce, F., Cormio, A., Bufo, P., Carrieri, G., & Cormio, L. (2015). Molecular markers in bladder cancer: Novel research frontiers. *http://dx.doi.org/10.3109/10408363.2015.1033610*, 52(5), 242–255.
<https://doi.org/10.3109/10408363.2015.1033610>
58. Siegel, R. L., Miller, K. D., Fuchs, H. E., & Jemal, A. (2022). Cancer statistics, 2022. *CA: A Cancer Journal for Clinicians*, 72(1), 7–33. <https://doi.org/10.3322/CAAC.21708>
59. Sud, M., Fahy, E., Cotter, D., Brown, A., Dennis, E. A., Glass, C. K., et al. (2007). LMSD: LIPID MAPS structure database. *Nucleic Acids Research*, 35(SUPPL. 1). <https://doi.org/10.1093/nar/gkl838>
60. Sun, N., Liang, Y., Chen, Y., Wang, L., Li, D., Liang, Z., et al. (2019). Glutamine affects T24 bladder cancer cell proliferation by activating STAT3 through ROS and glutaminolysis. *International Journal of Molecular Medicine*, 44(6), 2189–2200. <https://doi.org/10.3892/IJMM.2019.4385/HTML>
61. Sung, H., Ferlay, J., Siegel, R. L., Laversanne, M., Soerjomataram, I., Jemal, A., & Bray, F. (2021). Global Cancer Statistics 2020: GLOBOCAN Estimates of Incidence and Mortality Worldwide for 36 Cancers in 185 Countries. *CA: A Cancer Journal for Clinicians*, 71(3), 209–249. <https://doi.org/10.3322/CAAC.21660>
62. Swanson, M. G., Keshari, K. R., Tabatabai, Z. L., Simko, J. P., Shinohara, K., Carroll, P. R., et al. (2008). Quantification of choline- and ethanolamine-containing metabolites in human prostate tissues using 1H HR-MAS total correlation spectroscopy. *Magnetic Resonance in Medicine*, 60(1), 33–40.
<https://doi.org/10.1002/MRM.21647>
63. Tan, G., Wang, H., Yuan, J., Qin, W., Dong, X., Wu, H., & Meng, P. (2017). Three serum metabolite signatures for diagnosing low-grade and high-grade bladder cancer. <https://doi.org/10.1038/srep46176>
64. Tayebati, S. K., Martinelli, I., Moruzzi, M., Amenta, F., & Tomassoni, D. (2017). Choline and Choline alphascerate Do Not Modulate Inflammatory Processes in the Rat Brain. *Nutrients*, 9(10), 1084.
<https://doi.org/10.3390/NU9101084>
65. Tripathi, P., Somashekar, B. S., Ponnusamy, M., Gursky, A., Dailey, S., Kunju, P., et al. (2013). HR-MAS NMR tissue metabolomic signatures cross-validated by mass spectrometry distinguish bladder cancer from benign disease. *Journal of Proteome Research*, 12(7), 3519–3528.
https://doi.org/10.1021/PR4004135/SUPPL_FILE/PR4004135_SL001.PDF
66. Vance, J. E., & Tasseva, G. (2013). Formation and function of phosphatidylserine and phosphatidylethanolamine in mammalian cells. *Biochimica et Biophysica Acta (BBA) - Molecular and Cell Biology of Lipids*, 1831(3), 543–554. <https://doi.org/10.1016/J.BBALIP.2012.08.016>
67. Vantaku, V., Donepudi, S. R., Piyarathna, D. W. B., Amara, C. S., Ambati, C. R., Tang, W., et al. (2019). Large-scale profiling of serum metabolites in African American and European American patients with bladder cancer reveals metabolic pathways associated with patient survival. *Cancer*, 125(6), 921–932.
<https://doi.org/10.1002/CNCR.31890>
68. Wishart, D. S., Tzur, D., Knox, C., Eisner, R., Guo, A. C., Young, N., et al. (2007). HMDB: the Human Metabolome Database. *Nucleic Acids Research*, 35(Database), D521–D526.
<https://doi.org/10.1093/nar/gkl923>
69. Wittmann, B. M., Stirdivant, S. M., Mitchell, M. W., Wulff, J. E., McDunn, J. E., Li, Z., et al. (2014). Bladder Cancer Biomarker Discovery Using Global Metabolomic Profiling of Urine. *PLOS ONE*, 9(12), e115870.
<https://doi.org/10.1371/JOURNAL.PONE.0115870>

70. Wong, M. C. S., Fung, F. D. H., Leung, C., Cheung, W. W. L., Goggins, W. B., & Ng, C. F. (2018). The global epidemiology of bladder cancer: a joinpoint regression analysis of its incidence and mortality trends and projection. *Scientific Reports 2018 8:1*, 8(1), 1–12. <https://doi.org/10.1038/s41598-018-19199-z>
71. Wu, J. Y., Huang, T. W., Hsieh, Y. T., Wang, Y. F., Yen, C. C., Lee, G. L., et al. (2020). Cancer-Derived Succinate Promotes Macrophage Polarization and Cancer Metastasis via Succinate Receptor. *Molecular cell*, 77(2), 213-227.e5. <https://doi.org/10.1016/J.MOLCEL.2019.10.023>
72. Zeki, Ö. C., Eylem, C. C., Reçber, T., Kir, S., & Nemutlu, E. (2020). Integration of GC–MS and LC–MS for untargeted metabolomics profiling. *Journal of Pharmaceutical and Biomedical Analysis*, 190, 113509. <https://doi.org/10.1016/J.JPBA.2020.113509>
73. Zhang, X. W., Li, Q. H., Xu, Z. Di, & Dou, J. J. (2020). Mass spectrometry-based metabolomics in health and medical science: a systematic review. *RSC Advances*, 10(6), 3092–3104. <https://doi.org/10.1039/C9RA08985C>

Figures

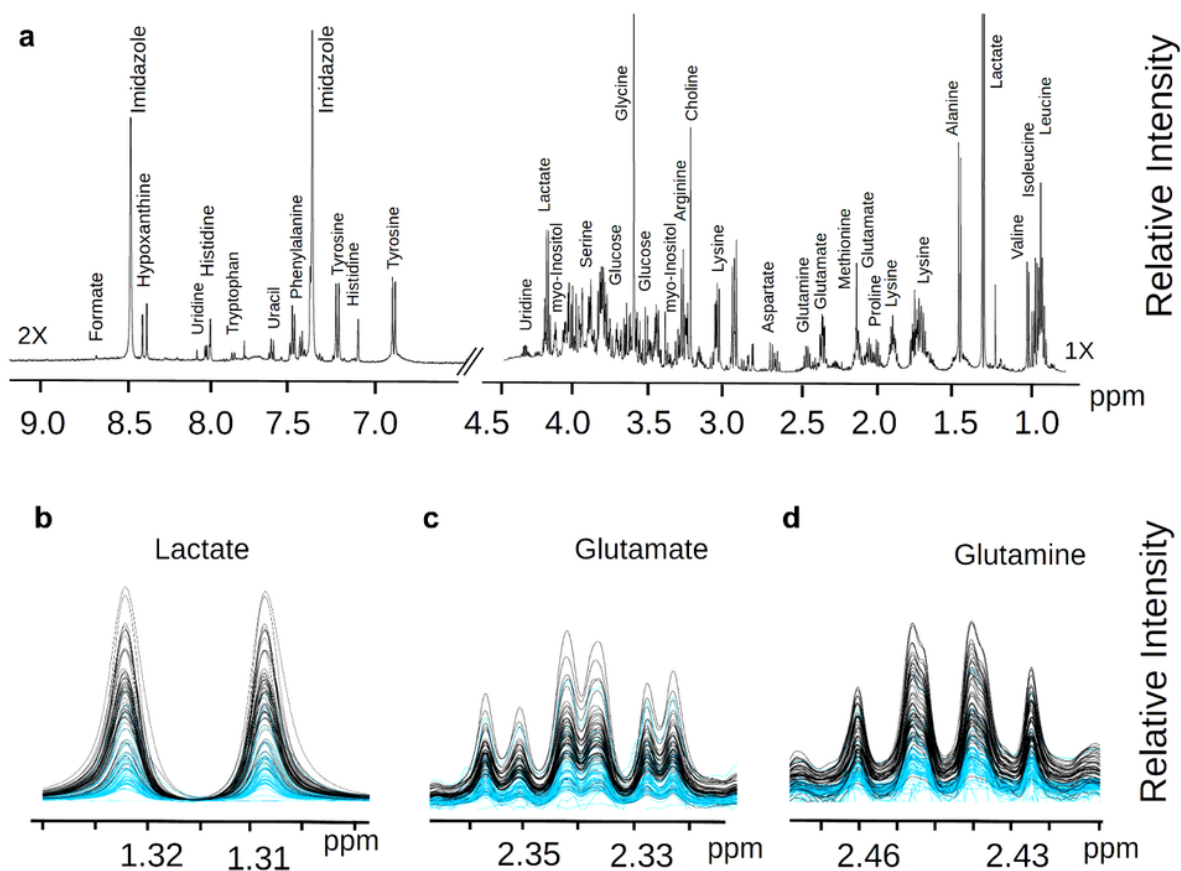


Figure 1

Representative 1D ^1H -NMR spectra of metabolites extracts obtained from cancerous versus healthy tissue of bladder cancer (BC) patients. (a) Full 1D ^1H NMR spectrum of a bladder cancer (BC) patient metabolite sample recorded on MSU 600 MHz (14 Tesla) solution NMR spectrometer. The chemical shift locations of several

identified metabolites in the tissue metabolite extracts of BC patients compared to healthy (normal) controls are labeled. Panel A depicts the overlays of ^1H NMR spectra from BC patient tissue samples (black) and control tissue samples (blue) are shown. Expanded regions of the spectra are shown in (b) for the chemical shift region 1.33-1.30 ppm corresponding to lactate; (c) for the chemical shift region 2.37-2.31 ppm corresponding to glutamate; and (d) for the chemical shift region 2.48-2.41 ppm corresponding to glutamine. The weight-normalized spectral overlays clearly indicate that the levels of these metabolites are higher in the cancer tissue of the BC patients compared to the levels found in the healthy tissue controls.

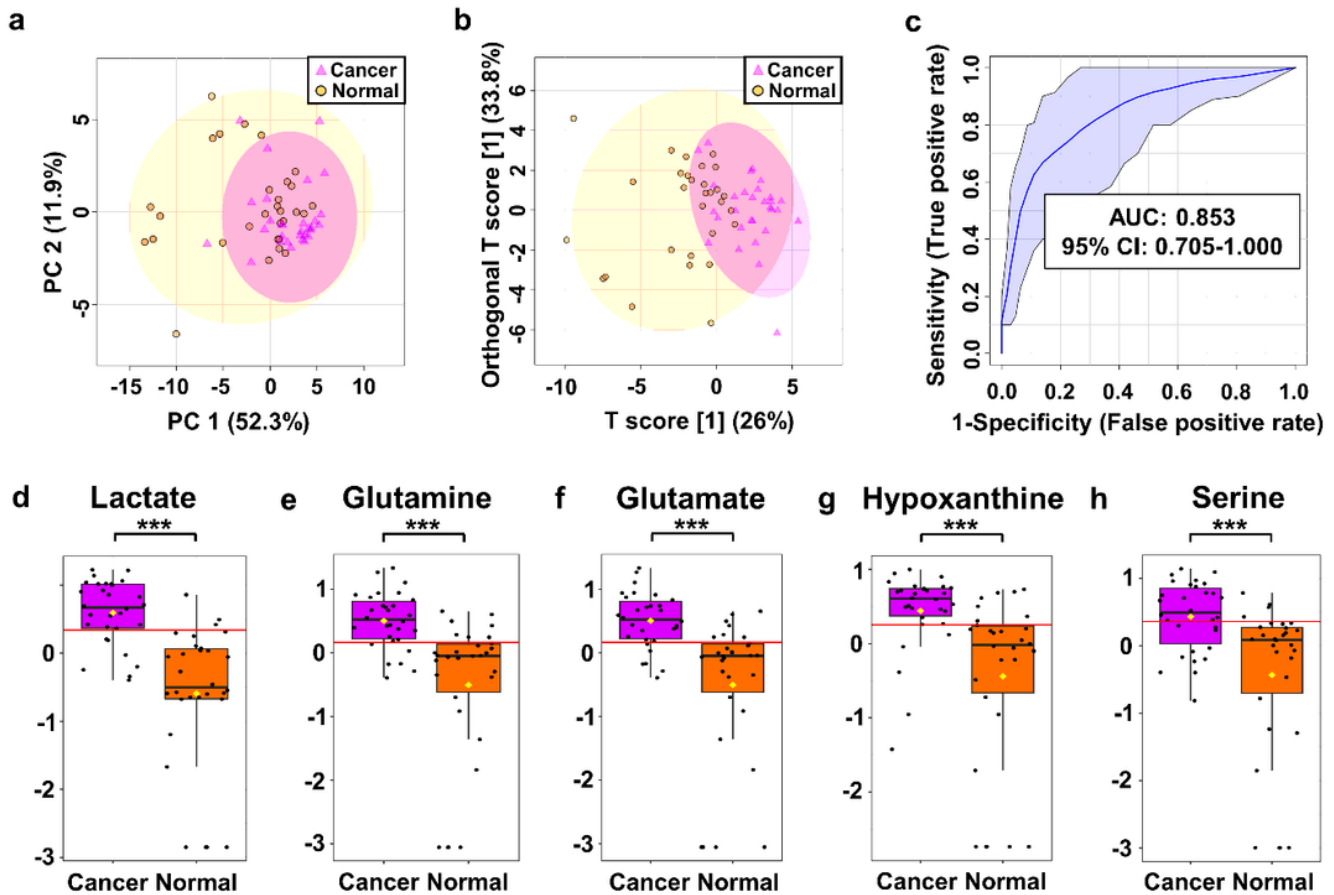


Figure 2

Cancer and normal tissue metabolite profiles obtained from ^1H NMR data distinguish BC and AN samples in the training set. (A,B) The tumor (violet) and normal (orange) tissue samples were evaluated using (a) 2D PCA, and (b) OPLS-DA scores. (c) ROC curves of six distinct metabolites: lactate, glutamine, glutamate, hypoxanthine, serine and threonine. (d-h) Box-whisker plots of selected metabolites levels in tissue samples from NCs and AN. AUC: area under the curve; PC: primary component; ROC: the receiver operator characteristic

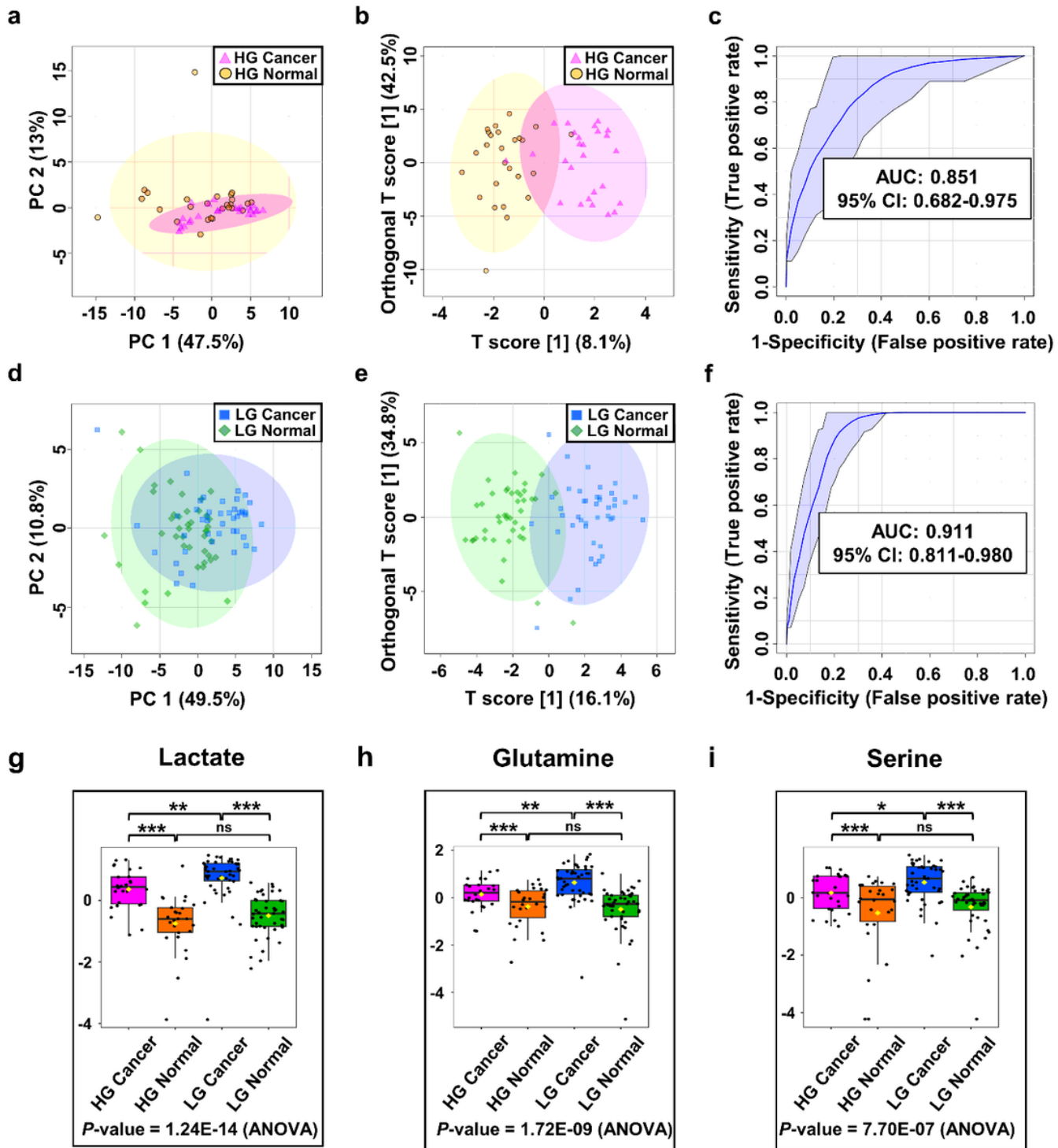


Figure 3

Analysis of the tissue metabolite profiles obtained from the ^1H NMR training dataset and assessment of whether metabolite differences can be used to differentiate between various grades of bladder cancer and normal tissue samples. (a) PCA and (b) OPLS-DA score plots of HG BC (violet) and AN (orange) tissue samples. (c) ROC curves of the two most differentiating HG BC metabolites. (d) PCA and (e) OPLS-DA score plots of LG BC (green) and AN (orange) tissue samples. (f) ROC curves of the eleven most differentiating LG BC metabolites. (g - i) The box-and-whisker plots of selected metabolites were observed in the control, HG, and LG

BC urine samples. AN: adjacent normal; AUC: area under the curve; HG: high grade; LG: low grade; PC: primary component; ROC: the receiver operator characteristic;

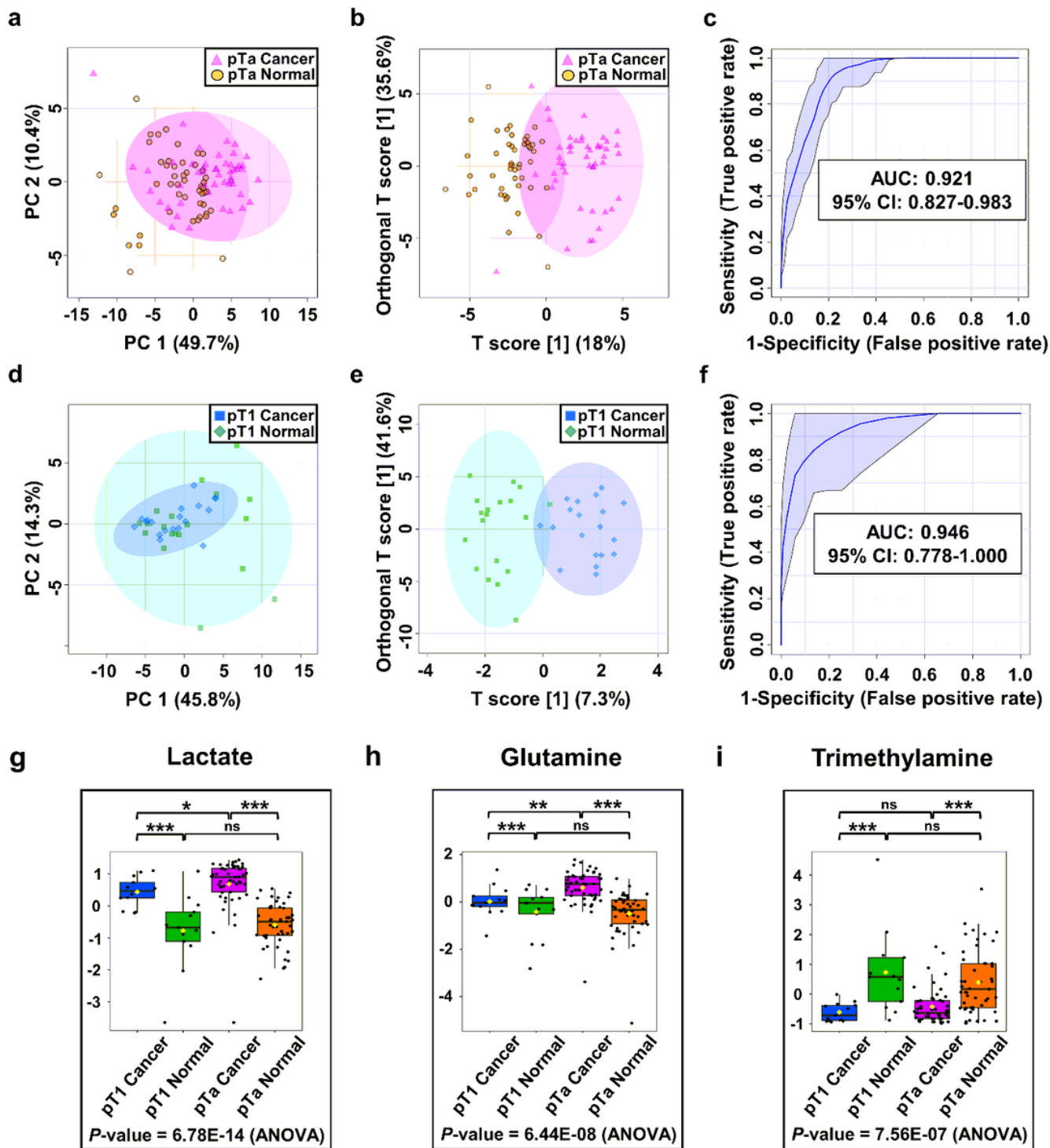


Figure 4

Analysis of the tissue metabolite profiles obtained from the ^1H NMR training dataset and assessment of whether metabolite differences can be used to differentiate between various stages of bladder cancer and normal tissue samples. (a) PCA and (b) OPLS-DA score plots of pTa BC (violet) and AN (orange) tissue samples. (c) ROC curves of the twelve most differentiating pTa BC metabolites. (d) PCA and (e) OPLS-DA score

plots of pT1 BC (green) and AN (orange) tissue samples. (f) ROC curves of the two most differentiating pT1 BC metabolites. AN: adjacent normal; AUC: area under the curve; PC: primary component; ROC: the receiver operator characteristic

Supplementary Files

This is a list of supplementary files associated with this preprint. Click to download.

- [BCTkankiNMRLDIMSupplementary.docx](#)
- [BCTkankiNMRLDIMSupplementary.docx](#)